Solvent-dependent conformational polymorphism in the crystal structure of mercuric bromide adduct of 1,1′-bis(diphenylphosphino)ferrocene

Bahareh Tamaddoni Jahromi [a], Ali Nemati Kharat [a] & Abolghasem Bakhoda [b]

[a] School of Chemistry, University College of Science, University of Tehran, Tehran, Iran

[b] Department of Chemistry, Southern Illinois University, Edwardsville, IL, USA

Accepted author version posted online: 07 May 2013.Published online: 11 Jun 2013.

PLEASE SCROLL DOWN FOR ARTICLE

Taylor & Francis
Taylor & Francis Group

Solvent-dependent conformational polymorphism in the crystal structure of mercuric bromide adduct of 1,1′-bis(diphenylphosphino)ferrocene

BAHAREH TAMADDONI JAHROMI†, ALI NEMATI KHARAT*† and
ABOLGHASEM BAKHODA‡

†School of Chemistry, University College of Science, University of Tehran, Tehran, Iran
‡Department of Chemistry, Southern Illinois University, Edwardsville, IL, USA

Two polymorphs of dinuclear mercury–iron complexes, [HgBr$_2$(dppf)] (**1**) where dppf is 1,1′-bis(diphenylphosphino)ferrocene, are prepared and crystal structures are determined by X-ray crystallography. The reaction of mercury(II) bromide with dppf in methanol–dichloromethane led to orange block polymorph. After crystallization of this complex in DMSO, a red needle polymorph was obtained.

Keywords: Polymorph; **1**; 1′-Bis(diphenylphosphino)ferrocene; Mercuric bromide; X-ray Crystallography

1. Introduction

Polymorphism, the ability of a molecule to crystallize in more than one packing arrangement, is an important chemical and crystallographic phenomenon [1–11]. Polymorphs can be generally recognized by different unit cell parameters and often from the different crystal symmetries. The occurrence of polymorphs implies that the free energies of the various crystalline forms are comparable [12, 13]. Polymorph formation upon crystallization is generally sensitive to variation in conditions such as temperature, type of solvent, pressure, and the manner in which the crystals are obtained [14]. Reproducibly obtaining a specific polymorph of a given compound can be a critical issue for proper formulation of pharmaceuticals, dyes, explosives, and pigments [15–17]. Polymorphism results when different (but energetically similar) packing interactions are operative during crystal growth.

Here, we describe two X-ray crystal structures of a complex that exhibit conformational polymorphism. The dimorphs **1** and **2** are supramolecular complexes with ferrocene moiety that show weak CH···Br hydrogen bonding in their packing. Crystallization of the complex in THF or a mixture of ethanol–dichloromethane (EtOH : DCM) leads to orange crystals, whereas crystallization in DMSO gives a mixture of orange and red crystals.

---

*Corresponding author. Email: alnema@khayam.ut.ac.ir

Polymorphs arise from differences in the relative orientation of phenyl rings of diphenyl-phosphine groups of the flexible dppf in the complex. This phenomenon is not known for coordination complexes of mercury(II) halides (chloride and iodide) with dppf as ligand [18, 19].

2. Experimental

2.1. *Materials and instrumentation*

Preparation and purification of **1** and **2** were carried out under an atmosphere of dry nitrogen. Solvents were deoxygenated prior to use and dried and distilled over appropriate drying agents. 1,1'-Bis(diphenylphosphino)ferrocene (dppf) was purchased from Acros and used without purification. Mercury(II) bromide, dichloromethane, methanol, THF, DMSO, and DMSO-d_6 were purchased from Merck. Melting points were determined with an Electrothermal 9200 melting point apparatus. Infrared spectra from 250 to 4000 cm^{-1} were recorded on a Shimadzu 470 FT-IR instrument using CsI pellets. ^{31}P NMR spectra were recorded at room temperature in DMSO-d_6 on a Bruker AVANCE 300 MHz. The ^{31}P NMR spectra were referenced to H$_3$PO$_4$ 85% as external standard. Crystalline samples suitable for single-crystal X-ray diffraction were grown by slow evaporation of THF or methanol–dichloromethane solution of complex for orange crystals and slow vapor diffusion of methanol in concentrated DMSO solution of complex for both red and orange crystals.

2.2. *Crystallography*

The X-ray diffraction measurements were made on a Nonius Kappa-CCD diffractometer with graphite monochromated Mo-K$_\alpha$ radiation. For **1** and **2**, orange block crystal with a dimension of $0.26 \times 0.14 \times 0.12$ mm and needle red crystal of $0.24 \times 0.12 \times 0.10$ mm, respectively, was mounted on a glass fiber and used for data collection. Cell constants and an orientation matrix for data collection were obtained by least-squares refinement of diffraction data from 5275 for **1** and 5107 for **2** unique reflections. Data were collected at a temperature of 150(2) K to a maximum 2θ value of 55.06° for **1** and 55.02° for **2** and in a series of ω scans in 1° oscillations and integrated. The data were corrected for Lorentz and polarization effects. The structures were solved by direct methods [20] and subsequent difference Fourier maps and then refined on F^2 by a full-matrix least-squares procedure using anisotropic displacement parameters [20].

2.3. *Synthesis of polymorph 1*

HgBr$_2$ (0.1 g, 0.277 mmol) was dissolved in 10 mL methanol and a solution of dppf (0.154 g, 0.277 mmol) in 10 mL dichloromethane was added all at once; the resulting clear orange solution was stirred vigorously at room temperature for 30 min. The orange precipitate was filtered off and the orange mother liquor was kept at room temperature. Orange block crystals were obtained after a few days, collected, and dried under vacuum (0.128 g, yield = 62%), m.p. = 301 °C (dec).

A second reaction was performed in a manner analogous to previous part where $HgBr_2$ and dppf were dissolved in THF and orange blocks of polymorph **1** were obtained. Yield = 43% (0.089 g).

2.4. *Synthesis of polymorph 2*

To get more crystalline sample of [$HgBr_2$(dppf)], the orange precipitate of the complex [$HgBr_2$(dppf)] (0.128 g) from the previous section was first washed with cold methanol and then with dichloromethane and finally dissolved in hot DMSO. The color of solution changed from bright orange to brownish-orange after 20 min. Unexpectedly, orange block crystals of **1** with a slight amount of red needles of polymorph **2** were obtained after 5 days by slow diffusion of methanol vapor to DMSO solution of the complex. The yield for orange crystals was 77% (0.098 g) and for red crystals was 9% (0.012 g). m.p. = 289 °C (dec.) for red crystals.

3. Results and discussion

[$HgBr_2$(dppf)] (**1**) was prepared by reaction of $HgBr_2$ with dppf in methanol–dichloromethane, scheme 1. The $^{31}P\{^1H\}$NMR spectrum of the [$HgBr_2$(dppf)] in DMSO-d_6 solution shows a triplet at 14.12 ppm with $^1J(^{199}Hg\text{-}^{31}P) = 499$ Hz. X-ray quality crystals were grown by slow evaporation from the mother solution. Single-crystal X-ray diffraction of **1** shows a monoclinic (*C2/c*) system. After recrystallization of **1** in hot DMSO, a slight amount of red crystals with triclinic (*P*ī) system were obtained (polymorph **2**), scheme 1. The crystallographic data of **1** and **2** are listed in table 1. ORTEP diagrams of **1** and **2** are shown with their atom numbering scheme in figure 1. The most significant bond lengths and angles of **1** and **2** are presented in table 2.
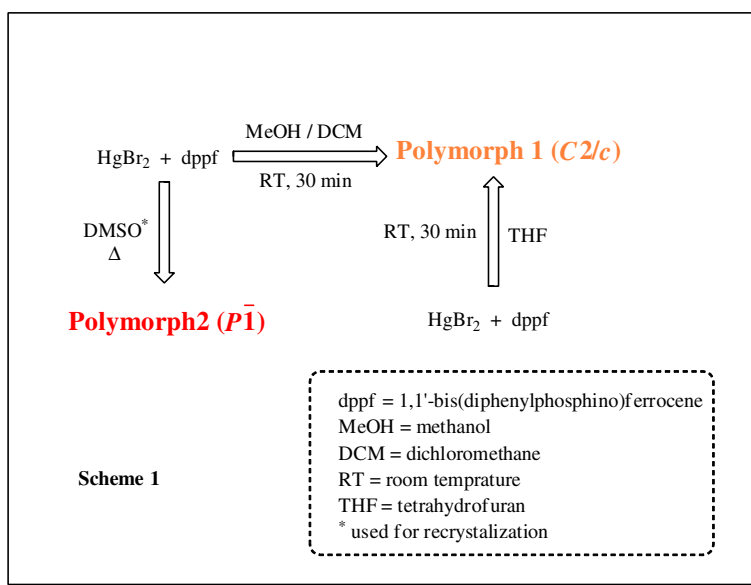
Scheme 1. Synthesis route for preparation of **1** and **2**.

Table 1. Crystallographic and structure refinement data for polymorphs **1** and **2**.

Polymorph	**1**	**2**
Formula	$C_{34}H_{28}Br_2FeHgP_2$	$C_{34}H_{28}Br_2FeHgP_2$
Formula weight	914.76	914.76
Temperature/K	150(2)	150(2)
Wavelength λ/Å	0.71073	0.71073
Crystal system	Monoclinic	Triclinic
Space group	*C2/c*	*P*ī
Crystal size/mm^3	$0.26 \times 0.14 \times 0.12$	$0.10 \times 0.12 \times 0.24$
a/Å	33.8737(11)	9.7345(4)
b/Å	10.0467(2)	10.0226(4)
c/Å	18.4571(6)	18.2223(7)
α/°	90.00	97.938(2)
β/°	98.8590(15)	98.516(2)
γ/°	90.00	116.286(2)
Volume/Å^3	6206.4(3)	1534.29(11)
Z	8	2
Density (calc.)/g cm^{-1}	1.958	1.980
θ ranges for data collection	2.7–27.53	2.7–27.5
F(000)	3504	876
Absorption coefficient/mm^{-1}	8.110	8.202
Index ranges	$-42 \leqslant h \leqslant 43$	$-12 \leqslant h \leqslant 12$
	$-12 \leqslant k \leqslant 12$	$-12 \leqslant k \leqslant 12$
	$-23 \leqslant l \leqslant 24$	$-19 \leqslant l \leqslant 23$
Data collected	17,912	20,111
Unique data (R_{int})	7046, (0.052)	6948, (0.079)
Parameters, restraints	361, 0	361, 0
Final R_1, wR_2^{a} (obs. data)	0.0375, 0.0718	0.0483, 0.0929
Final R_1, wR_2^{a} (all data)	0.0633, 0.0805	0.0834, 0.1073
Goodness of fit on F^2 (S)	0.0998	1.04
Largest diff. peak and hole/eÅ^3	1.655, -1.734	2.311, -1.749

$^a R_1 = \Sigma ||F_o|-|F_c||/\Sigma|F_o|$; $wR_2 = [\Sigma(w(F_o{}^2-F_c{}^2)^2)/\Sigma w(F_o{}^2)^2]^{1/2}$.
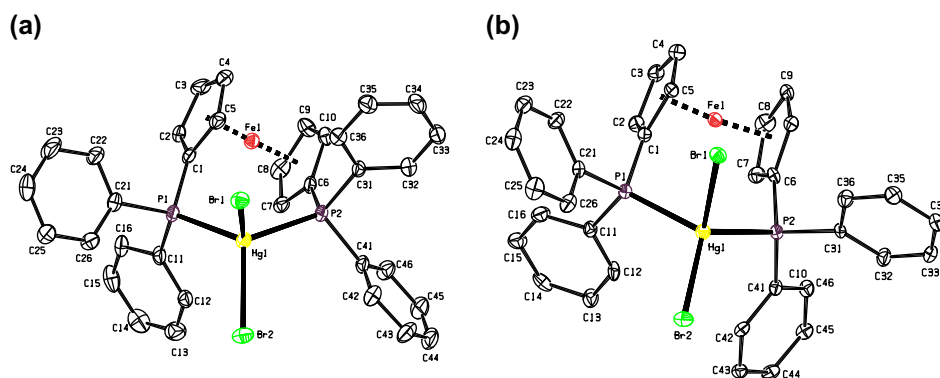

Figure 1. ORTEP plot drawn with 50% ellipsoidal probability showing the atom-labeling scheme. (a) Orange block form (polymorph **1**) and (b) red needle form (polymorph **2**). All hydrogens are omitted for clarity (see http://dx.doi.org/10.1080/00958972.2013.801960 for color version).

In **1**, the coordination geometry around mercury(II) is distorted tetrahedral from bidentate dppf and two bromides. All bond lengths and angles are in normal ranges. After recrystallization of **1** in hot DMSO, a slight amount of red crystals of **2** were obtained. The molecular structure of **2** is similar with **1** with mercury(II) coordinated to a bidentate dppf and two bromides.

Table 2. Most significant bond lengths and angles of **1** and **2** (Å and °).

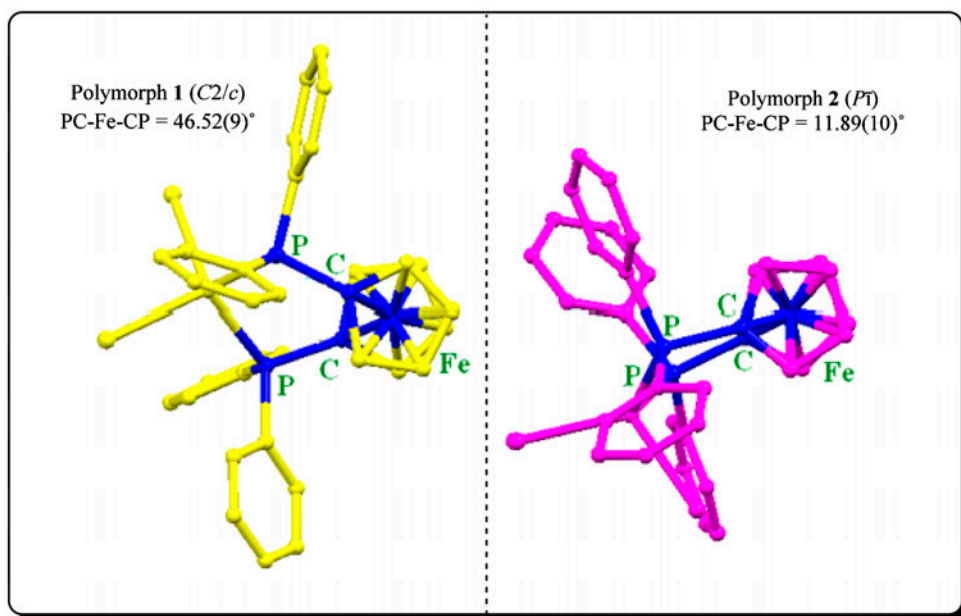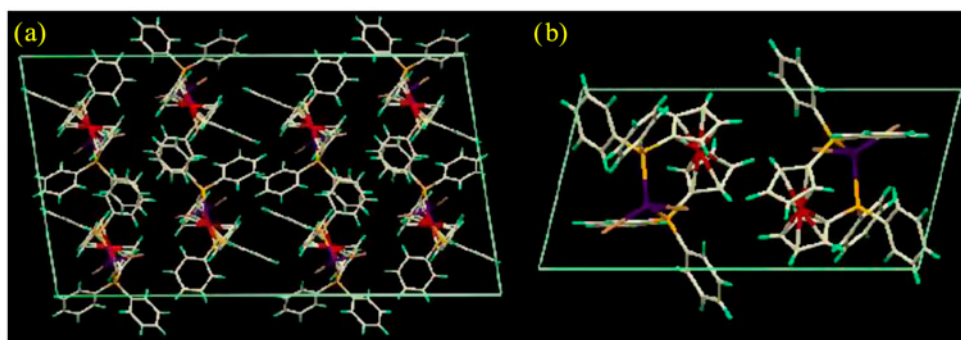| Polymorph	1	2
Bond length		
Hg(1)–Br(1)	2.617	2.667
Hg(1)–Br(2)	2.626	2.592
Hg(1)–P(1)	2.530	2.498
Hg(1)–P(2)	2.541	2.484
Bond angle		
Br(1)–Hg(1)–Br(2)	104.365	110.422
P(1)–Hg(1)–P(2)	108.364	108.720

Figure 2. The individual molecule of **1** (yellow) and **2** (purple) illustrate the conformational freedom of the flexible dppf (see http://dx.doi.org/10.1080/00958972.2013.801960 for color version).

Figure 3. Packing diagram of (a) orange polymorph (**1**) and (b) red polymorph (**2**) (see http://dx.doi.org/10.1080/00958972.2013.801960 for color version).

Table 3. C–H···Br hydrogen bond parameters of **1** and **2** in crystal packing (Å, °).

D–H···A	D–H	H···A	D···A	D–H···A	Sym. code
Polymorph **1**					
C3-H3A···Br1	0.999	2.881	3.746	145	*X*, −1 + *Y*, *Z*
C4-H4A···Br1	1.000	3.006	3.840	142	½ −*X*, −½ + *Y*, ½ −*Z*
C44-H44A···Br2	0.952	3.001	3.857	151	−*X*, *Y*, ½ −*Z*
Polymorph **2**					
C9-H9A···Br1	1.000	2.976	3.952	166	1 −*X*, 1 − *Y*, 1 − *Z*
C14-H14A···Br2	0.951	3.028	3.720	131	1 −*X*, 1 − *Y*, −*Z*
C35-H35A···Br1	0.951	2.987	3.722	135	2 −*X*, 1 − *Y*, 1 − *Z*
C45-H45A···Br1	0.951	2.987	3.683	131	*X*, 1 + *Y*, *Z*
C45-H45A···Br2	0.951	2.953	3.670	133	*X*, 1 + *Y*, *Z*

The independent molecules observed in the dimorphs of **1** differ in their angle between the P–C–Fe mean planes of coordinated dppf. The conformational differences between the two polymorphic modifications are shown in figure 2. The conformation of each dppf with respect to iron may be defined according to the PC–Fe–PC angle. Conformational changes from one structure to the other lead to formation of two different polymorphs. In order to establish whether conformational changes were the reason for the polymorphism, we plotted two diagrams as shown in figure 2. The packing of these polymorphs (figure 3) is stabilized by weak intermolecular C–H···Br hydrogen bonding, listed in table 3.

4. Conclusion

In the present contribution, we have shown that polymorphism plays an important role in structural chemistry of [HgBr$_2$(dppf)] and allows us to compare structure of compounds exhibiting the same chemical composition but with different arrangement of their building blocks.

Supplementary data

CCDC 778306 and 778307 contain the supplementary crystallographic data for **1** and **2**. These data can be obtained free of charge from The Cambridge Crystallographic Data Center via http://www.ccdc.cam.ac.uk/data_request/cif.

Acknowledgment

References

[1] J. Dunitz, J. Bernstein. *Acc. Chem. Res.*, **28**, 193 (1995).
[2] A. Nangia. *Acc. Chem. Res.*, **41**, 595 (2008).
[3] N. Blagden, R.J. Davey. *Cryst. Growth Des.*, **3**, 873 (2003).

[4] B.M. Kukovec, Z. Popović. *J. Mol. Struct.*, **938**, 174 (2009).
[5] D. Braga, F. Grepioni. *J. Chem. Soc., Chem. Commun.*, 571 (1996).
[6] G. Labat, N.R. Behrnd, G. Couderc, M. Bonin, J. Tsuwi, A. Batagiannis, R. Berger, M. Bertoni, A. Prodi-Schwab, J. Hulliger. *Cryst. Eng. Comm.*, **12**, 1252 (2010).
[7] G.R. Desiraju. *Science*, **278**, 404 (1997).
[8] I.S. Konovalova, S.V. Shishkina, B.V. Paponov, O.V. Shishkin. *Cryst. Eng. Comm.*, **909**, (2010).
[9] P.K. Thallapally, R.K.R. Jetti, A.K. Katz, H.L. Carrell, K. Singh, K. Lahiri, S. Kotha, R. Boese, G.R. Desiraju. *Angew. Chem. Int. Ed.*, **278**, 1149 (2004).
[10] D. Tzimopoulos, A. Czapik, M. Gdaniec, T. Bakas, A.A. Isab, A.C. Varvogli, P.D. Akrivos. *J. Mol. Struct.*, **965**, 56 (2010).
[11] D. Das, E. Engel, L.J. Barbour. *Chem. Commun.*, **10**, 1676 (2010).
[12] X. Zheng, B. Wang, U. Englert, G.E. Herberich. *Inorg. Chem.*, **40**, 3117 (2001).
[13] D. Braga, F. Grepioni. *Chem. Soc. Rev.*, **29**, 229 (2000).
[14] A. Karmakar, R.J. Sarma, J.B. Baruah. *Eur. J. Inorg. Chem.*, **643**, (2007).
[15] V.S.S. Kumar, F.C. Pigge, N.P. Rath. *New J. Chem.*, **27**, 1554 (2003).
[16] D. Chopra, T.P. Mohan, K.S. Raob, T.N.G. Row. *Cryst. Eng. Comm.*, **374**, (2005).
[17] R.K. Harris. *Angew. Chem. Int. Ed.*, **45**, 6609 (2006).
[18] Y.Y. Niu, Y.L. Song, S.X. Liu, X.Q. Xin. *Z. Anorg. Allg. Chem.*, **628**, 179 (2002).
[19] J. McGinley, V. McKee, C.J. McKenzie. *Acta Cryst.*, **C54**, 345 (1998).
[20] G.M. Sheldrick. *Acta Crystallogr.*, **A64**, 112 (2008).